

### Inter-Dendrimer Stabilized Ag/Au Alloy and Core-Shell Nanoparticles

Hossein Nanaie\*, Associate Professor, Claflin University, [hnanai@claflin.edu](mailto:hnanai@claflin.edu)

Alicia Cooper, Student, Claflin University, [alicia.cooper@claflin.edu](mailto:alicia.cooper@claflin.edu)

Shameka Sanders, Student, Claflin University, [shameka.sanders@claflin.edu](mailto:shameka.sanders@claflin.edu)

Donggao Zhao, Assistant Professor, University of South Carolina, [dzhao@sc.edu](mailto:dzhao@sc.edu)

#### Abstract

Ag/Au alloy and Ag/Au core-shell nanoparticles (NPs) stabilized by Generation 4 PAMAM (Polyamidoamine) dendrimer were synthesized in aqueous solution. The alloy was prepared by the reduction of mixtures of metal ions using NaBH<sub>4</sub>. The plasmon resonance absorption bands of the mixture NPs were red shifted as  $\chi_{Au}$  increased indicating alloy formation. The concentration dependent average diameter was  $2.92 \pm 0.57$  nm at  $\chi_{Au} = 0.50$ . The core-shell composites were prepared by reducing Au<sup>+3</sup> with ascorbic acid in solution containing silver NPs seeds. The characteristic surface plasmon absorption of silver NPs at about 400 nm in the seed solution was progressively weakened with the incremental addition of 0.1 mM HAuCl<sub>4</sub> in the presence of ascorbic acid and ultimately vanished completely. The disappearance of Ag plasmon absorption was accompanied by the growth, intensification and red shifting of gold NPs absorption reaching a  $\lambda_{max}$  of 576 nm at  $\chi_{Au} = 0.75$ . HRTEM dark field mode image shows that core-shell composite NPs with average diameter of  $14.5 \pm 2.7$  nm are produced, when Ag seeds are allowed to stand 30 minutes at room temperature before capped with Au. Reducing the standing time to 5 minutes, the average particle diameters decreases to  $6.2 \pm 1.5$  nm.

#### Introduction

The study of particles of nanoscale dimensions has drawn much attention due to the size-dependent novel properties that they exhibit<sup>1</sup>. In the last decade, attention has been focused on functionalizing nanoparticles (NPs) by highly branched polymeric molecules with three dimensional structures called dendrimers to create self-assembled metal nanoparticles<sup>2</sup>. Extensive research has been directed toward synthesis and characterization of alloy and core-shell nanostructured metal particles to understand the influence of bimetalization on optical, electronic and catalytic properties<sup>3</sup>. Interest in the dependence of optical properties on the molar ratios of the metals in Ag/Au nano-alloy and core/shell structures and the existence of solid surface resonance plasmon absorption of Ag and Au in the visible spectral range have invited extensive research activity. In many of these studies various generations of Poly (amidoamine) PAMAM dendrimers were used for their templating effects. Dendrimers functionalize the metal NPs through both the interior and peripheral functional groups<sup>4</sup>. By varying the peripheral functional groups metal ions may be directed into the interior of the dendrimer where chemical reduction leads to formation of NPs<sup>5-7</sup>. The metal NPs that are formed at the surface of dendrimer are stabilized by the peripheral amino groups. These NPs are larger than the intradendrimer particles primarily due to limited space for the latter particles to grow. There is ample evidence that NPs can be encapsulated both in the internal void space<sup>8</sup> as well as the periphery or branch points of the dendrimer<sup>9</sup>. In this paper we report the preparation of Au/Ag alloy and Ag/Au core/shell NPs by chemical reduction and their characterization by their plasmon resonance absorption spectra and transmission electron microscopy. We have used fixed concentration of generation 4 amino-terminated PAMAM dendrimer to template the alloy and core/shell NPs. Attempts, however, to produce Au-core Ag-shell structure by this method failed.

---

\* Corresponding author

## Experimental Section

**Materials.** Fourth generation amino-terminated PAMAM dendrimer as 10% solution in methanol, L-ascorbic acid (99%), and  $\text{HAuCl}_4 \cdot 3 \text{H}_2\text{O}$  (99.9%) were purchased from Aldrich Chemical Co. (Milwaukee, WI).  $\text{NaBH}_4$  (99%) and  $\text{AgNO}_3$  (99%), were purchased from Fisher Scientific. All chemicals were used without further purification. Distilled water (18 M $\Omega$ .cm) was used in all preparations. Solutions of  $\text{HAuCl}_4 \cdot 3 \text{H}_2\text{O}$  were prepared from a 0.254 mM stock solution protected from light. Weighed amount of  $\text{NaBH}_4$  was dissolved in chilled water immediately before use in every preparation and  $\text{AgNO}_3$  solutions were freshly prepared and kept in brown containers. Methanol in 10% of G4.NH<sub>2</sub> PAMAM dendrimer in methanol was evaporated by a stream of ultra pure nitrogen gas flowing over the solution until the dendrimer remained behind as a viscous liquid. Stock aqueous solutions in 0.1 mM regimes were then prepared.

**Characterization.** UV-vis spectra were recorded in a Shimadzu Model UV-2401 PC spectrophotometer and cuvettes having a 1.00-cm path length at room temperature. The changes in the surface plasmon optical signatures of the as prepared composite nanoparticles were correlated with the variations in the composition. Morphological characteristics of the preparations were examined by electron microscopy. HRTEM images were taken in a Jeol model 2100F high resolution transmission electron microscope operating at 200 kV. Samples were deposited on 200 mesh carbon-coated nickel grids by placing a drop of the solution on the grid and allowing it to evaporate to dryness at room temperature.

**Preparation of Au/Ag Alloy NPs.** Solutions of Ag and Au mixtures of various molar ratios were prepared from freshly prepared stock solutions. The total metal ions concentration was kept constant at 2.0 mM in all mixtures. NPs were synthesized by stepwise addition of calculated volumes of the as-prepared solution of metal precursors and dendrimer stock solution in enough distilled water to make up a total volume of 10-mL. The final solution in every run was 0.01 mM in dendrimer and 0.2 mM in metal ions. The ratio of  $\text{Ag}^+$  and  $\text{Au}^{3+}$  was varied as needed. The solution was then vigorously stirred after the addition of every component. Vigorous stirring was continued for 5 minutes before an excess of ice cold freshly prepared solution of  $\text{NaBH}_4$  was added (100  $\mu\text{L}$  of 0.10M  $\text{NaBH}_4$ ). Solution changed color immediately but stirring was continued for an additional 5 minutes. The color of solutions were dependent on the Ag/Au ratios in the mixtures that fall between the yellow-brown color of pure silver NPs to pink color of pure gold NPs.

**Preparation of Ag/Au Core/Shell NPs.** Core-shell bimetallic composites of silver and gold NPs were synthesized by seed-mediated technique<sup>10</sup>. Ag seed solution was prepared by diluting 2.0 mL of 1.0mM freshly prepared stock solution of Ag in 9 mL of distilled water and placed in a 20 mL beaker. A calculated volume of dendrimer in water was added to this solution with constant stirring. The final volume was adjusted to 10.0 mL with additional amount of distilled water. In this solution, the final concentrations of dendrimer and  $\text{AgNO}_3$  were 0.01 mM and 0.2 mM, respectively. While stirring, 100  $\mu\text{L}$  of 0.10 M  $\text{NaBH}_4$  was added to the solution. The reduction of  $\text{Ag}^+$  is slow and therefore stirring was continued for 5 to 15 minutes until the yellow-brown color of Ag NPs was fully developed. The aging time of silver seeds synthesized is crucial in controlling the size of the aggregates. The solution turns pink within 25 minutes of formation of NPs and becomes blue shortly afterward followed by complete aggregation leading to the formation of large particles which finally settled by gravity. In two different preparations, after allowed aging times of 5 and 30 minutes, a 100  $\mu\text{L}$  of 0.10 M freshly prepared ascorbic acid was added and solution was titrated with 0.1mM  $\text{HAuCl}_4$  by the incremental addition of 250  $\mu\text{L}$  of the solution with constant stirring. The fast reduction of  $\text{Au}^{3+}$  ions by the remaining of the excess  $\text{NaBH}_4$  initially added to produce Ag seeds will be followed by a slow one with ascorbic acid. Slower rate of reduction by ascorbic acid is preferred because it prevents the formation of pure Au aggregates and produces a uniform gold shell over Ag seeds. With each addition, the yellow-brown color of silver NPs changed and finally gave way to pink color of gold NPs. The aggregation of Ag seeds stops immediately after adding the first drop of  $\text{HAuCl}_4$  to the solution. The addition was then slowed down with confidence for thorough mixing. The UV-vis spectrum was recorded after each addition.

## Results and Discussion

**Ag/Au alloy NPs.** Ag/Au alloy NPs at various gold mole fractions,  $\chi_{\text{Au}}$ , coated with amino terminated generation 4 PAMAM dendrimer were synthesized in solution. At milli-molar concentrations used in this work, no AgCl precipitation occurred when  $\text{AgNO}_3$  and  $\text{HAuCl}_4$  were mixed. The equilibrium concentration of free  $\text{Cl}^-$  is very small in solution due to incomplete dissociation of  $\text{AuCl}_4^-$  complex ion in water<sup>11</sup>. Solutions were slightly turbid at highest mole fraction of  $\text{HAuCl}_4$  prior to reduction but became clear thereafter. The plasmon absorption spectra of NP alloys at various  $\chi_{\text{Au}}$ , and a plot of  $\lambda_{\text{max}}$  against  $\chi_{\text{Au}}$  are illustrated in figures 1 and 2, respectively. Both figures illustrate a red shift for the alloy plasmon band with increasing  $\chi_{\text{Au}}$ . By considering the uncertainties in locating  $\lambda_{\text{max}}$  due to the broadness of the absorption bands (figure 1), a slight deviation from straight line in figure 2 is justified and therefore ignored. The data of this study are in agreement with the theoretical calculations of extinction spectra of Ag/Au nanoparticles using Mie theory<sup>12</sup> which produced a linear relationship between  $\lambda_{\text{max}}$  and  $\chi_{\text{Au}}$ . Additionally, from this data it is clear that the reduction of mixtures of gold and silver precursors in the presence of generation 4 amino terminated PAMAM dendrimer form NPs with a single Plasmon band which is a function of composition of the alloy. It is also evident from figure 1 that red shift is more pronounced at lower  $\chi_{\text{Au}}$  and bands become more closely spaced with increasing  $\chi_{\text{Au}}$  demonstrating that the position of  $\lambda_{\text{max}}$  for alloy is not a simple average of those for pure Ag and Au NPs. The increasing plasmon bandwidth with increasing Au concentration, as noted in figure 1, may be explained in terms of increasing polydispersity in size illustrated in figures 3C and 3D for  $\chi_{\text{Au}}$  of 0.33 and 0.50 as well as variation in shapes of the particles (figure 3E). Additional supporting evidence for alloy formation is provided by the spectrum of a 50-50 mixture of Ag and Au nanoparticles that were separately prepared. This spectrum marked Au/Ag in figure 1 (not normalized) exhibits two well defined bands at 400 nm and 530 nm corresponding to pure Ag and Au plasmon resonance absorptions, respectively. This feature is absent in the alloy bands.

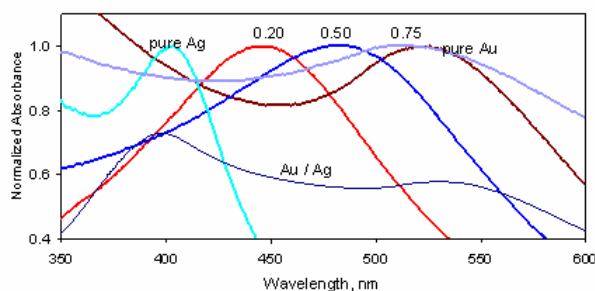


**Figure 1.** UV-vis Spectra of Au/Ag Alloy NPs at various mole fractions of Au that are shown on the curves. Mixed Ag and Au NPs are also shown.

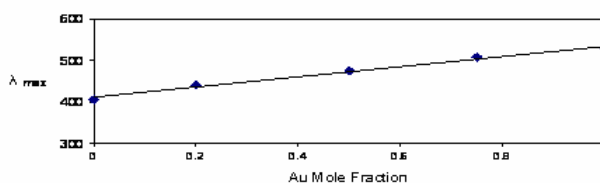


**Figure 2.** Wavelength of maximum absorption of Ag/Au alloy NPs as a function of Au mole fraction.

The slow formation of Ag and slightly more positive standard reduction potential of  $\text{AuCl}_4^-$  ( $E^\circ=1.002\text{V}$ ) than  $\text{Ag}^+$  ( $E^\circ = 0.7996\text{V}$ )<sup>13</sup> suggest that initially in the course of reduction of bimetal ionic mixture very small gold NPs seeds are formed. Subsequently, both metal ions are simultaneously adsorbed, reduced and deposited on the Au seeds surface forming an alloy shell. Apparently, alloying is a fast process that is catalyzed by gold NPs. A similar catalytic mechanism has been proposed for Pt NP-catalyzed formation of gold NPs<sup>14</sup>. In addition, since zero valent Au is believed to be less reactive toward aggregation than zero valent Ag<sup>15</sup>, we find that, although Ag nanoparticles easily aggregate in solution, alloying with gold is facilitating stronger coordination with primary amino groups of the dendrimer molecules producing stable bimetallic particles.

The resulting alloy NPs are less than 5 nanometers in diameter that varies with Au to Ag ratio. HRTEM results of figure 3 and particle size distribution graph in the same figure show the presence of relatively polydispersed alloy nanoparticles with an average diameter of  $2.92 \pm 0.57$  nm and  $3.52 \pm 0.67$  nm at  $\chi_{\text{Au}}$  of 0.33 and 0.50, respectively. The high resolution image along the direction of electron beam in 3E clearly shows that the particles are closer to hexagonal rather than spherical

shapes. The crystal structure of the particles is marked by the ordered lattice planes separated by 0.192 nm which may be assigned to (200) planes of fcc unit cell. At low resolution however the particles appear spherical and size distribution was determined on this assumption. No information can be provided by HRTEM to show the difference between the gold and silver atoms in the alloy nanoparticles. Very close unit cell constants for Au and Ag (4.0862 Å for silver and 4.0786 Å for gold<sup>13</sup>) is expected to bring about nearly perfect match in Au/Ag alloy.

The formation of nanoparticles larger than 1-2 nm and the polydispersity of alloy nanoparticles indicate that the particles are generated outside the dendrimer cavity and functionalized by the peripheral amino groups. Nanoparticles encapsulated within the dendrimer are small and uniform in size because the dendrimer cavity can hold a particular number of metal ions prior to the reduction and the particles formed will remain confined<sup>16</sup>. Once particles are formed, the steric effects inhibit their aggregation. The inter-dendrimer formation of silver-gold alloy NPs in generation 4 amino terminated PAMAM dendrimer is also ruled out empirically by the results of our experiment with generation 4 hydroxyl terminated dendrimer. We found that no spectroscopically distinguishable alloy is formed when a mixture of H<sub>2</sub>AuCl<sub>4</sub> and AgNO<sub>3</sub> was reduced in the presence of hydroxyl terminated generation 4 PAMAM dendrimer. Small templated gold particles, however, were observed in this reaction but silver and Ag/Au alloy NPs were not present. Silver is absent from the long list of metal ions that can be sequestered into dendrimer cavity by interacting with interior tertiary amines<sup>17</sup> which can be subsequently reduced to the corresponding metal nanoparticles.

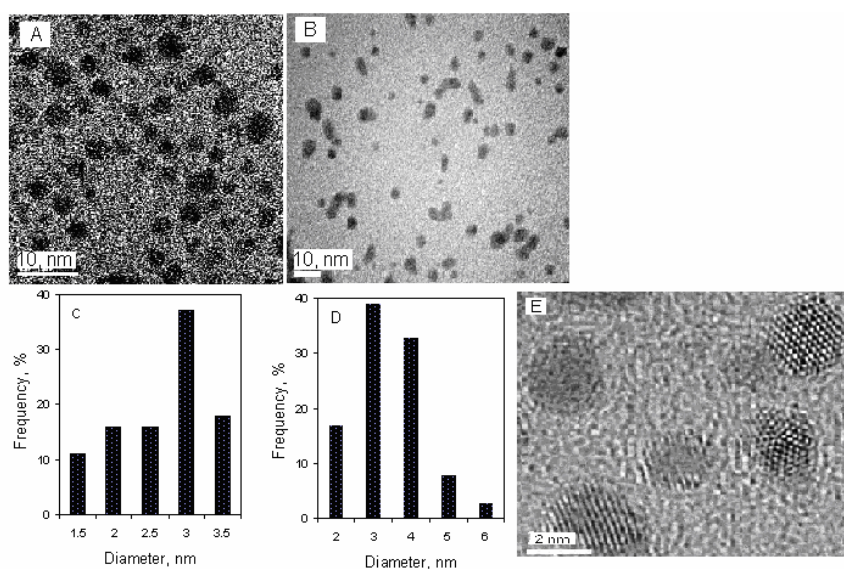


**Figure 3.** HRTEM images of Au/Ag alloy NPs. (A)  $\chi_{Au} = 0.33$ , particle diameter  $2.92 \pm 0.57$  nm (B)  $\chi_{Au} = 0.50$ , particle diameter  $3.52 \pm 0.67$  nm. (C) and (D) show size distribution for HRTEM images of NPs in (A) and (B). (E) High magnification image of alloy nanoparticles. Measured lattice plane spacing is 0.192 nm.

**Au/Ag core/shell NPs.** The first step in the synthesis of Ag core and Au shell NPs is preparing Ag seed NPs. The Ag seed formation in this system is a slow reaction taking about 5-10 minutes to obtain fully grown Ag NPs showing well developed plasmon absorption band at 400 nm. Solution is faintly yellow at start with its weak absorption band at about 375 nm. With time, the band intensity increases and red shifted to 400 nm. Kinetic studies of nucleation of silver nanoparticles have shown that after a short induction period of 5 minutes nucleation ensues followed by a sudden rise in the growth rate which is complete within 20 minutes<sup>18</sup>. The growth can be arrested by the addition of gold NPs precursor at any time after the initial formation period and during the rapid ripening process. The UV-vis absorption spectra of the solution show clear changes as Au nanoparticles are deposited on the surface of Ag seeds. Surface plasmon band of Ag at 400 nm decreases in intensity by incremental addition of Au precursor with a concomitant appearance of alloy NPs band at a wavelength which

depends on the amount of  $\text{HAuCl}_4$  added. At equimolar concentration, Ag seeds are partially covered by Au and thus the absorption bands of both metals are present. At higher gold concentrations ( $\text{Au}^{+3}$  mole fraction of 0.75) silver plasmon band completely disappears and a single broad band at 576 nm emerges as illustrated in figure 4. This band is assigned to gold plasmon resonance absorption and the red shift and broadening may be attributed to large size and polydispersity of the particles.

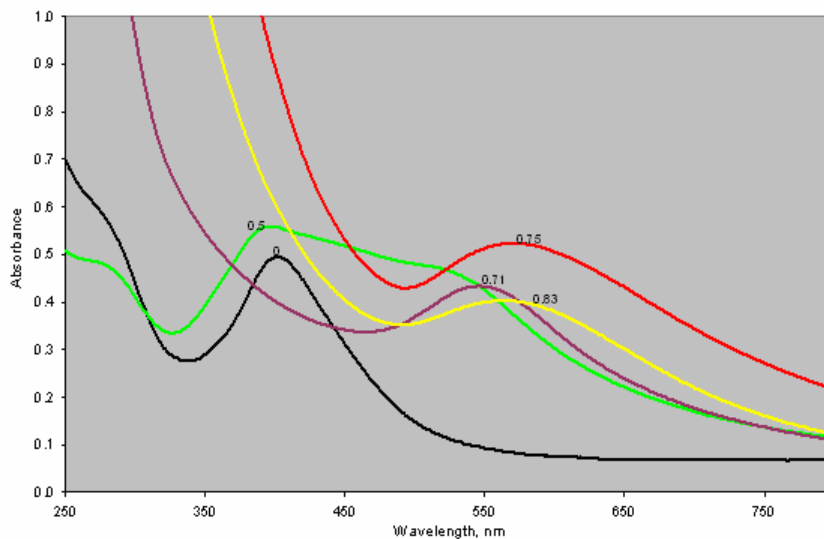


**Figure 4.** UV-Vis absorption spectra of solutions of Ag-core Au-shell nanoparticles at various mole fractions. Number on each curve give  $\text{Au}^{3+}$  mole fraction.

HRTEM micrographs of core/shell NPs at a mole fraction of 0.75 for  $\text{Au}^{+3}$  are shown in figure 5. Silver seeds that were allowed to stand for 20 minutes prior to capping with gold gave rise to large aggregates of  $14.5 \pm 2.7$  nm in diameter as illustrated in figure 5A. The size distribution shown in figure 5C, indicates that the aggregates are also polydispersed. It is also evident from the micrographs that the particles are uniformly covered by gold cap. At higher surface gold concentrations corrugation may occur as it has been observed<sup>19</sup> previously but we avoided excess coverage to prevent pure Au formation. The dependence of plasmon band maximum on the gold shell thickness and the stability of the particles makes this composite tunable for certain optical applications requiring accurately known wavelengths.

Particle size and polydispersity of silver particles are directly related to the degree of aggregation. We were able to control and manipulate the aggregation of silver seeds substantially in this work by influencing the growth times of silver seeds. Thus the micrograph in figure 5B shows particles with  $6.2 \pm 1.5$  nm diameters produced by depositing gold shell on silver seeds that were aged for 5 minutes. This procedure resulted in a narrow particle size distribution as shown in figure 5D. Published results for the preparation of core-shell composites involving silver seeding have pointed to the formation of large size particles. Mirkin<sup>19</sup> and his group have reported the synthesis of surface corrugated seed mediated Au shell Ag core NPs with diameter of  $21.5 \pm 3.6$  nm at  $\text{Ag}^+/\text{Au}^{3+}$  concentration ratio of 1/5 and obtained larger particles at higher ratios. In this work, we kept this ratio below 1/3 and  $\text{Au}^{3+}$  concentrations low (0.1 mM regimes). Dong<sup>20</sup> prepared silver seed mediated Ag-Au nanoshells using tri-sodium citrate to reduce and stabilize 100 nm aggregates. More recently, Ag seed mediated Ag-Au nanocomposites with core/shell structure stabilized by poly(vinylpyrrolidone) were found to be 7.9 nm in diameter<sup>21</sup>. The tendency for the formation of large silver NP seed may be explained by the slow rate of reduction, reactivity of zero valent  $\text{Ag}^{14}$  toward aggregation described above and in particular the inter-dendrimer formation of Ag NPs due to the yielding structure of the dendrimer in this work. Attempt to obtain higher surface coverage by the addition of more gold resulted in unwanted pure Au nanoparticle formation.

Gold shell of small silver seeds of this type is perfectly uniform as shown by equally spaced lattice planes (0.276 nm) which are assigned to (111) planes (figure 5E). Core-shell NPs are formed in various shapes as shown in 5E octahedral or polyhedral of higher order.

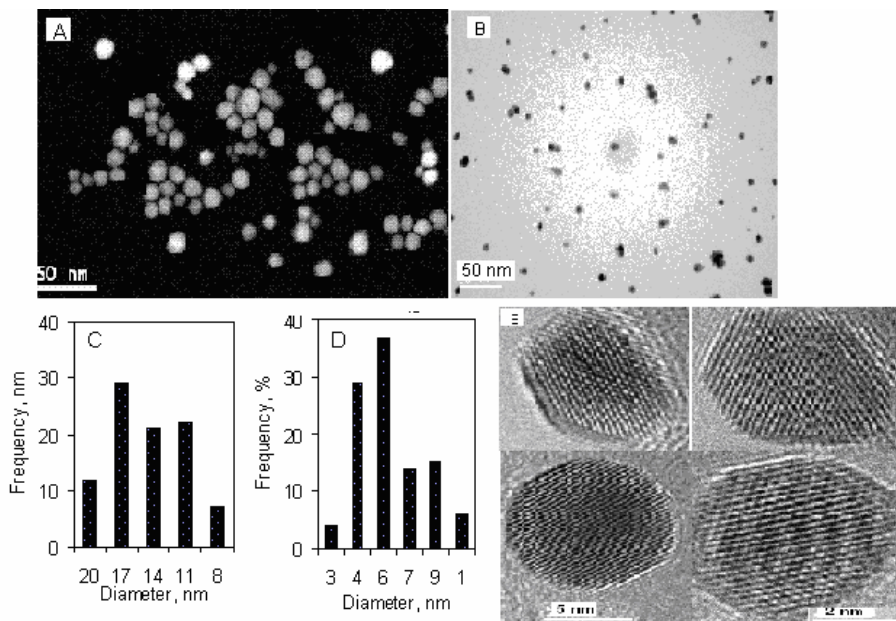


**Figure 5.** HRTEM images of Ag/Au core-shell NPs at  $\chi_{Au} = 0.75$ : (A) Ag NPs seeds were aged for 30 min and capped with Au, particle diameter  $14.5 \pm 2.7$  nm. Dark field mode (B) Ag NPs seeds were aged for 5 min and capped with Au, particle diameter  $6.2 \pm 1.5$  nm. (C) and (D) show size distribution for HRTEM images of NPs in (A) and (B). (E) high magnification for variously shaped nanoparticles with lattice plane distance of 0.276 nm.

## Summary and Conclusion

In conclusion, we report the synthesis of alloy and core-shell of silver and gold metal nanoparticles stabilized with generation 4 amino-terminated PAMAM dendrimer. We were able to establish simple and reproducible procedures to synthesize core-shell and alloyed nanostructures with controllable size and the optical properties which are uniquely dependent on the stoichiometric ratios of the two metals precursors. In this work the size of core-shell structures was controlled by two different and independent procedures. In one procedure, the silver seeds were allowed to stand for a given amount of time followed by capping with a shell of gold nanoparticles. In a second procedure, the as prepared silver seeds were covered with multiple gold shells as needed to obtain the desired size. Synthesis of nanoparticles with predetermined and controlled size and shape is very important for tuning the optical, chemical, physical and catalytic properties to a particular application.

## References

1. (a) Alivisatos, A.P., *J. Phys. Chem.* 1996, *100*, 13226. (b) Schmid, G. In *Clusters and Colloids. From Theory to Applications*; VCH: Weinheim, 1994. (c) Jana, N.R.; Sau, T.K.; Pal, T. *J. Phys. Chem. B* 1999, *103*, 115. (d) Gates, B.C.; Geuezi, L.; Knosinger, H. *Metal Clusters in Catalysis*; Elsevier; Amsterdam, 1986.
2. (a) Bosman, A. W.; Janssen, H. M.; Meijer, E. W. *Chem. Rev.* 1999, *99*, 1665. (b) Endo, T.; Yoshimura, T.; Esumi, K. *J. Colloid Interface Sci.* 2005, *286*, 602. (c) Narayanan, R.; El-Sayed, M. A. *J. Phys. Chem. B* 2004, *108*, 8572. (d) Scott, R. W. J.; Ye, H.; Henriquez, R. R.; Crooks, R. M. *J. Chem. Mater.* 2003, *15*, 3873.

3. (a) Sao-Joao, S.; Giorgio, S.; Penisson, J. M.; Chapon, C.; Bourgeois, S.; Henry, C. *J. Phys. Chem. B* 2005, 109, 342. (b) Mandal, S.; Selvakannan, P. R.; Pasricha, R.; Sastry, M., *J. Am. Chem. Soc.* 2003, 125, 8440. (c) Esumi, K.; Matsumoto, T.; Seto, Y.; Yoshimura, T. *J. Colloid Interface Sci.* 2005, 284, 199. (d) Mulvaney, P.; Giersig, M.; Henglein, A. *J. Phys. Chem.* 1993, 97, 7061. (e) Michaelis, M.; Henglein, A.; Mulvaney, P. *J. Phys. Chem.* 1994, 98, 6212.
4. Crooks, R. M.; Lemon, B. I., III; Sun, L.; Yeung, L. K.; Zhao, M. *Topics in Current Chemistry* 2001, 212 (Dendrimers III), 81.
5. Scott, W. J.; Wilson, O. M.; Crooks, R. M., *J. Phys. Chem. B* 2005, 109, 692.
6. Zhao, M.; Crooks, R. M., *Adv. Mater.* 1999, 11, 3379.
7. Wilson, O. M.; Scott, R. W. J.; Jaquin, C.; Martinez G.; Crooks, R. M., *J. Am. Chem. Soc.* 2005, 127, 1015.
8. Scott R. W. J.; Wilson, O. M., Crooks, R. M., *J. Phys. Chem. B* 2005, 109, 692.
9. Garcia, M. E.; Baker L. A.; Crooks, R. M. *Anal Chem.* 1999, 71, 256.
10. (a) Gole, A.; Murphy, C. J., *Chemistry of Materials* 2004, 16, 3633. (b) Chandran, S. P.; Pasricha, R.; Bhatta, U. M.; Satyam, P. V.; Sastry, M., *J. Nanosci. Nanotechnol.* 2007, 7, 2808. (c) Berhaut, G.; Bausach, M.; Bisson, L.; Becerra, L.; Thomazeau, C.; Uzio, D., *J. Phys. Chem. C* 2007, 111, 5915.
11. Han, M. Y.; Quek, C. H., *Langmuir* 2000, 16, 362.
12. Moskovits, M.; Smova-Sloufova, I.; Vlkova, B, *J. Chem. Phys.* 2002, 116, 10435.
13. Lide, D. R., *Handbook of Chemistry and Physics*, CRC Press, Inc., 71<sup>st</sup> ed, New York 1991.
14. Njoki, P.N.; Jacob, Aisley; Khan, B.; Luo, J.; Zhong, C-J, *J. Phys. Chem. B* 2006, 110, 22503.
15. Manna, A.; Imae, T.; Aoi, K.; Okada, M.; Yogo, T., *Chem. Mater.*, 2001, 13, 1674.
16. Zhao, M.; sun L.; Crooks, R.M, *J. Am. Chem. Soc.* 1998, 99, 1665.
17. Crooks, R. M.; Zhao, M.; Chechik, V.; Yeung, L.K., *Acc. Chem. Res.*, 2001, 34, 181.
18. Patakfalvi, R; Papp, S. and Dekany, I., *J. Nanopart. Res.* 2007, 9, 353.
19. Sanedrin, R. G.; Georganopoulou, D. G.; Park, S.; Mirkin, C.A., *Adv. Mater.* 2005, 17, 1027.
20. Jin, Y.; Dong, S., *J. Phys. Chem. B* 2003, 107, 12902.
21. Yang, J.; Lee, J.Y.; Chen, L.X. and Too, Heng-Phon, *J. Nanosci. Nanotech.* 2005, 5, 1095.